Earthquake Geotechnical Engineering for Protection and Development of Environment and Constructions – Silvestri & Moraci (Eds)
© 2019 Associazione Geotecnica Italiana, Rome, Italy, ISBN 978-0-367-14328-2

Centrifuge model tests on improved soils using $Ca(OH)_2$ and SiO_2 grout

K. Uemura
Nippon Koei Co. ltd., Tokyo, Japan

R. Takatoku
Graduate school of Tokyo City University, Tokyo, Japan

K. Itoh & N. Suemasa
Tokyo City University, Tokyo, Japan

N. Kikkawa & N. Hiraoka
National Institute of Occupational Safety and Health, Tokyo, Japan

T. Sasaki
Kyokado Eng. Co., ltd, Tokyo, Japan

ABSTRACT: Properties of people have received terrible damage from liquefaction during large scale earthquakes in Japan. In this study, a new suspension grouting material which composed of fine silica particles and fine calcium hydroxide was developed for soil improvement and the effect on liquefaction countermeasure of the grout was investigated. In order to investigate dynamic behavior of structures on liquefiable sand and improved sand centrifuge modeling test was performed. From these results of experiments, it was confirmed that unimproved sand liquefied in each shaking event. On the other hand, decreasing of stiffness and area on hysteresis loop were not confirmed in the improved sand. Additionally, settlement in the improved sand was smaller than that in the liquefiable sand.

1 INTRODUCTION

In Japan, large earthquakes have occurred every few years and caused liquefaction in urban areas. In particular, properties of people received terrible liquefaction damage during the 2011 Tohoku earthquake, the 2016 Kumamoto earthquake and the 2018 Hokkaido Eastern Iburi earthquake. Therefore, it is highly necessary vital to develop an efficient countermeasure against liquefaction in such grounds. Generally, the solution type of chemical grout has been used for the liquefaction countermeasures for the ground under existing buildings (Gallagher et al. 2007). However, this type of grout requires accurate construction with controlling gel-time of grout precisely. Therefore, this gout is unsuitable for urban areas because low construction cost is demanded for improvement of these areas

In this study, a new suspension grouting material composed of fine SiO_2 particles (hereinafter referred to as Si) and fine particles of $Ca(OH)_2$(hereinafter referred to as CH) was proposed and its effect on preventing liquefaction was investigated. Micro particles used for the material are amorphous silica and fine calcium hydroxide. When these fine particles interact with each other, calcium silicate hydrate (C-S-H) is generated as a result of pozzolanic reaction and thereby the soil is reinforced. (Moue et al. 2018)

In this paper, in order to figure out liquefaction resistance of the grouting material composed of Si and CH, cyclic triaxial tests on improved sand were conducted. Secondly,

centrifuge modeling tests under 50G field were carried out to investigate behavior of structures on both liquefiable sand and improved sand during ground shaking for comparison.

2 CYCLIC TRIAXIAL TEST

2.1 *Test conditions*

A series of cyclic triaxial tests was performed to confirm liquefaction resistance of the sand improved by determined arrangement of grouting material. Test conditions are shown in Table 1. Silica sand No.6 was used for specimens and its physical properties and grain size are shown in Figure 1. Specimens of saturated sand were prepared by air-pluviation method at a relative density 60% and subsequently saturated by permeating de-air water. Specimens of improved sand were prepared by permeating the grouting material into sand specimens whose relative density was 60% and permeation pressure was set at 100 kPa to permeate it uniformly. The quantity and proportions of the grouting material were determined according to the results of previous study (Moue et al 2018). The fine particle content (P) was fixed at 0.10 by weight of water (W). And CH/Si is weight ratio between CH and Si. After cured for 7 days at 20°C, the prepared specimens were saturated in triaxial test apparatus and subsequently cyclic tests were started with subscribed cyclic shear stress ratio (hereinafter referred to as CSR).

2.2 *Test results*

The results of cyclic triaxial test are shown in Figure 2 where the relationship between number of cyclic when double amplitude (DA) of axial strain reached 5% and CSR is indicated. The liquefaction resistance of improved sand was approximately three times greater than that of

Table 1. Test conditions

Case No.	Test No.	Arrangements of grouting material		B-value	B.P. (kPa)	σ_0' (kPa)	$P/2A_c\sigma_0$'
		CH/Si	P/W				
Saturated specimen	a-1	-	-	0.95	100	100	0.151
	a-2	-	-	0.99	100	100	0.154
	a-3	-	-	0.96	100	100	0.162
	a-4	-	-	0.96	100	100	0.171
	a-5	-	-	0.95	100	100	0.177
Improved specimen	b-1	4/6	0.10	0.93	100	100	0.409
	b-2	4/6	0.10	0.93	100	100	0.497
	b-3	4/6	0.10	0.94	100	100	0.596
	b-4	4/6	0.10	0.94	100	100	0.696
	b-5	4/6	0.10	0.92	100	100	0.794

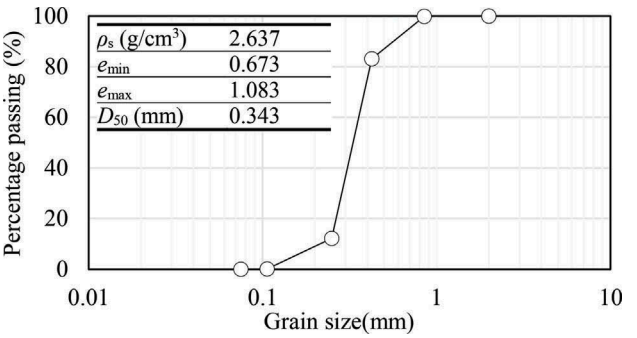

Figure 1. Grain size of silica sand No 6

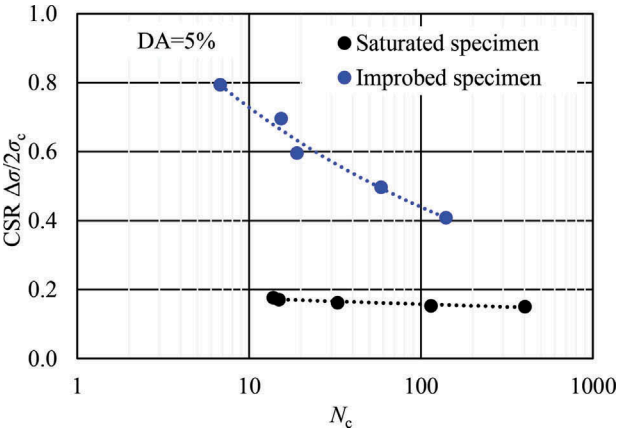

Figure 2. Liquefaction resistance

saturated sand. On the other hand, the B-values of improved sand were less than those of saturated sand. Yoshimi et al. (1989) and Okamura & Soga (2006) indicated that the smaller the B-value of specimen was, the larger the liquefaction strength was. On the other hand, Yoshimine et al. (1989) reported that the liquefaction resistance at 0.22 B-value is about 1.3 times that at full saturation. Therefore, it can be said that liquefaction resistance of improved sand is high enough for liquefaction countermeasure.

3 CENTRIFUGE TEST

3.1 *Summary of experiment*

In the centrifuge modeling tests, two types of specimens were used: liquefiable sand and sand improved by this grouting material. A laminar box is the flexible-wall soil container comprising a stack of rectangular aluminum frames separated by linear roller bearings which are arranged to permit relative movements between rings with minimal friction.

Air dried silica sand #6 was used for the model ground. As described in Figure 3, thickness of loose layer (D_r is approximately 60 %) and dense layer (D_r is approximately 80 %) were 170 mm and 80 mm (model type scale), respectively and vertical arrays of accelerometers and pore water pressure transducers were used for measurements. Conditions of specimens and sensors location on each case are shown in Figure 3(a) and (b). In the liquefiable sand (saturated sand), the specimen was prepared to become the prescribed relative densities by air-pluviation method. In the improved sand, the improved layer was arranged under a model structure. After prepared in the prescribed conditions, the specimens were successfully saturated and subsequently a model structure was loaded at the center of each ground surface.

A centrifugal model test system used in this study belongs to the National Institute of Occupational Safety and Health, Japan (JNIOSH). These centrifuge model tests were carried out under centrifugal acceleration field of 50G. Both specimens were subjected to three shaking events to evaluate liquefaction resistance. In-put acceleration waves were frequency 2.0Hz (prototype scale) as shown in Figure 4. In addition, in order to evaluate the responses of the models during the shakings, horizontal accelerations, pore water pressures in the soil, lateral displacements (D_L) of the frame and vertical displacement (D_V) of the soil or structures were measured.

3.2 *Experimental results*

These models were subjected to three shaking events to evaluate the difference in behavior between the saturated sand and the improved sand. All of the results from the centrifuge model tests were denoted with prototype scale hereafter.

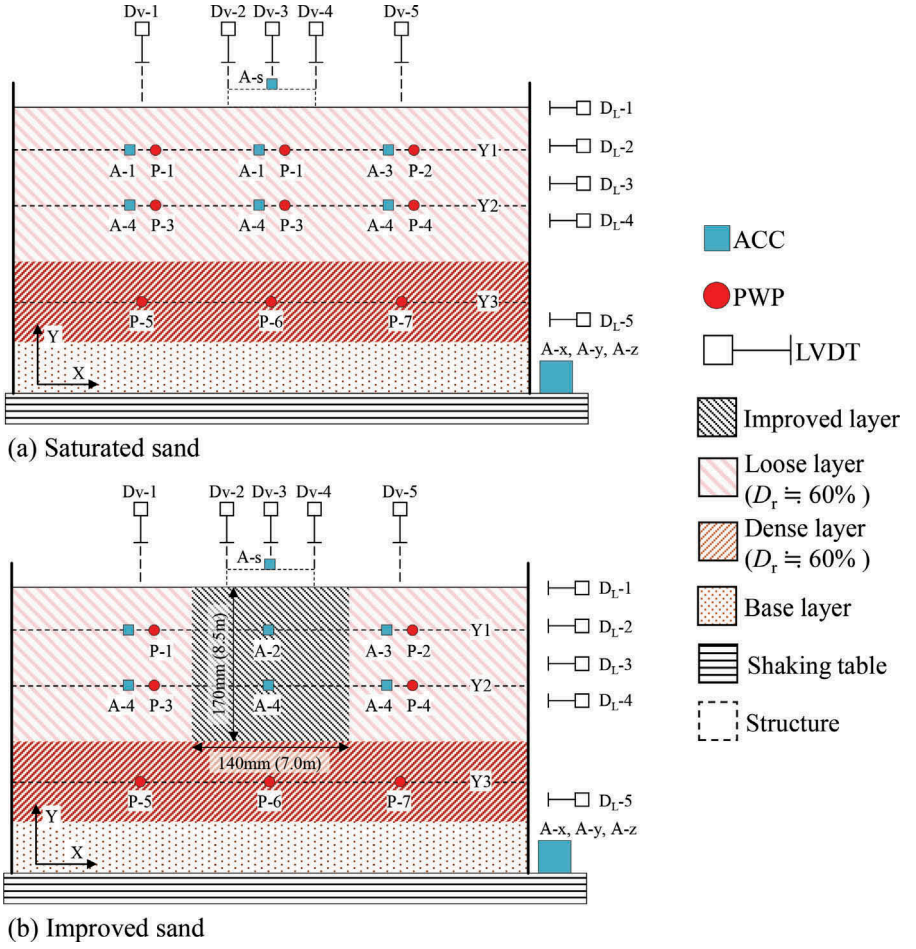

Figure 3. Sensors location

Table 2. Conditions of specimen

	D_r[%]			Sensors [pcs]			
	Loose	Dense	S_r [%]	ACC	PWP	LVDT	Bearing pressure (prototype) [kPa]
Saturated sand	58.3	79.5	99.9	11	9	10	24
Improved sand	57.7	84.5	99.2	11	6	10	24

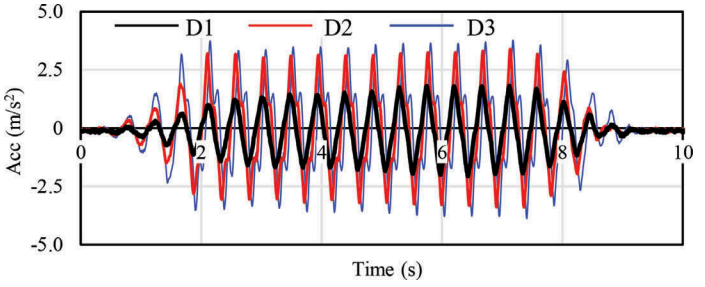

Figure 4. In-put wave recorded by A-x

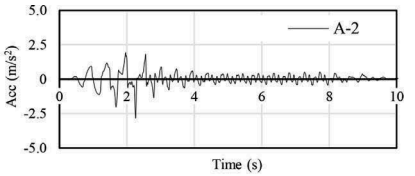

(a) Saturated sand A-2

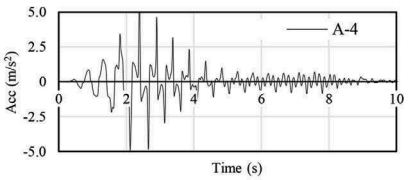

(b) Saturated sand A-4

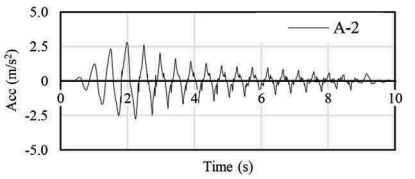

(c) Improved sand A-2

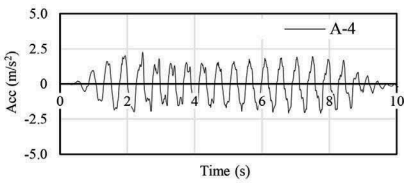

(d) Improved sand A-4

Figure 5. Recorded acceleration during third shaking event (D3)

3.2.1 *Recorded horizontal accelerations*

In this section, the recorded accelerations during the third shaking event (D3) were considered. Figure 5 (a) ~ (d) show the time histories of accelerations during the shaking. The response accelerations of the saturated sand decreased due to liquefaction. On the other hand, the amplitude of recorded acceleration of the improved sand (A-4) was constant, which indicated that the improved sand did not liquefy during the shaking. Additionally, it was presumed that the amplitude of acceleration of the improved sand (A-2) decreased due to the liquefaction occurred in adjacent unimproved layer.

3.2.2 *Response of pore water pressure*

Excess pore water pressure ratios (hereinafter referred to as EPWP ratios) were obtained from recorded EPWP divided by effective vertical stress σ'_v at its measured point as equation (1), to which structures bearing pressure σ_s derived from elastic theory by Boussinesq was added.

$$\text{EPWP ratio} = \frac{\text{EPWP}}{\sigma'_v + \sigma_s} \tag{1}$$

Figure 6 and Figure 7 show the contours of EPWP ratio for the saturated sand and the improved sand, respectively at the times selected from the whole time records when applying weakest shaking event (D1). Deep red denotes liquefaction (EPWP ratio = 1) and deep blue indicates that EPWP ratios are nearly zero. Moreover, the EPWP ratios in the improved layer

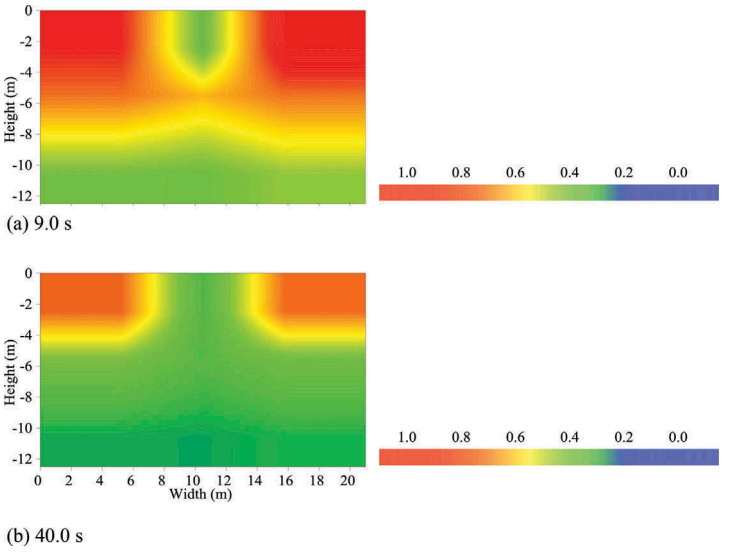

Figure 6. EPWP ratio on Saturated sand

were postulated zero. In Figure 7, the EPWP at upper left had not been recorded due to malfunction of P-1 during the centrifuge tests.

These contours indicated that liquefaction occurred in the upper layer first and propagated toward the bottom layer of the specimen. Moreover, the whole loose layer in the saturated sand except for the part under the structure completely liquefied by 9.0 s. The behavior of EPWP ratios in the improved sand was almost the same as that of the saturated sand but the magnitude of the improved sand was smaller than that of the saturated sand. The dissipation of pore waterpressure in upperboth sides in the saturated sand wasslow compared with the improvedsand since residual pore water pressure after liquefaction of bottom of saturated sandpropagated to its upper layer.

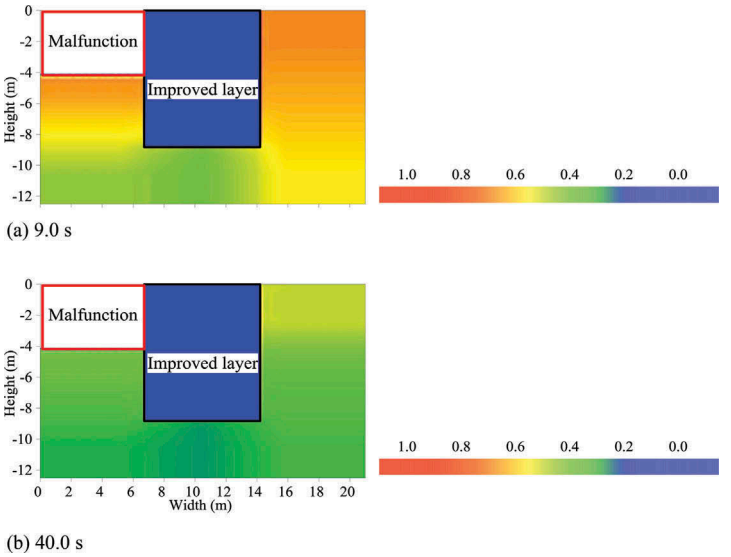

Figure 7. EPWP ratio on improved sand

3.2.3 *Relationship between shear strain and shear stress ratio*

Shear stress ratio (τ/σ'_0) and shear strain (γ) were calculated from equations (2) and (3), respectively. (Dietz & Wood 2007)

$$\frac{\tau}{\sigma'_o} = \frac{\rho_t H_i a_{xi}}{\sigma'_o} \tag{2}$$

$$\gamma(t) = \frac{\int\int (a_{x2}(t) - a_{x1}(t))dtdt}{H} \tag{3}$$

where ρ_t is the wet density of soil, H_i is the distance from ground surface to Yi, H is the distance from Y1 to Y2, a_{xi} is the recorded acceleration, and σ'_0 is the effective vertical stress, respectively. If shear wave propagated vertically, shear stress at the height of Hi can be calculated from multiplication of ρ_t, H and horizontal acceleration a_i. Additionally, in order to calculate shear deformation, the difference of accelerations recorded by the accelerometers arranged vertically were integrated twice.

The relationships between shear stress ratio and shear strain during the second shaking are shown in Figure 8 (a) ~ (d). In these figures, red, blue and green lines indicate hysteresis loops at the 2nd, 6th and 12th cycles on the second input wave (D2). In the saturated sand, the stiffness and area of hysteresis decreased during the second shaking event. On the other hands, the stiffness and hysteresis of shape of the improved sand was constant. From these results, it is presumed that the improved sand did not liquefy during the second shaking event.

3.2.4 *Settlement of ground surface*

Surface displacement before and after the shaking events in each case was measured by a laser displacement sensor as shown in Figure 9 where deep red and deep blue denote swell and settlement of surface, respectively, and the square formed by broken line indicate improved region.

The amount of settlement after shakings in the saturated sand was almost the same excluding the improved region. However, the structure settlement in the improved region was much smaller than that in the saturated sand.

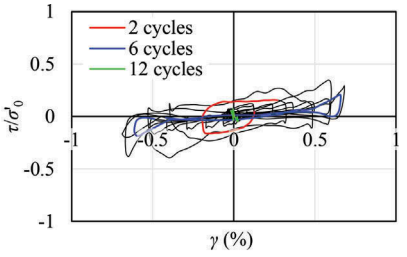

(a) Saturated sand A-1

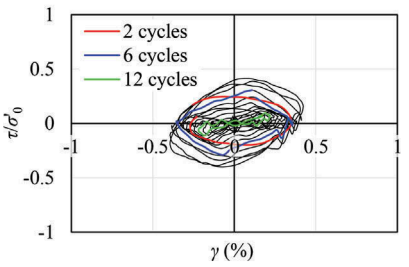

(b) Improved sand A-1

Figure 8. Relationships between τ/σ'_0 and γ on D2

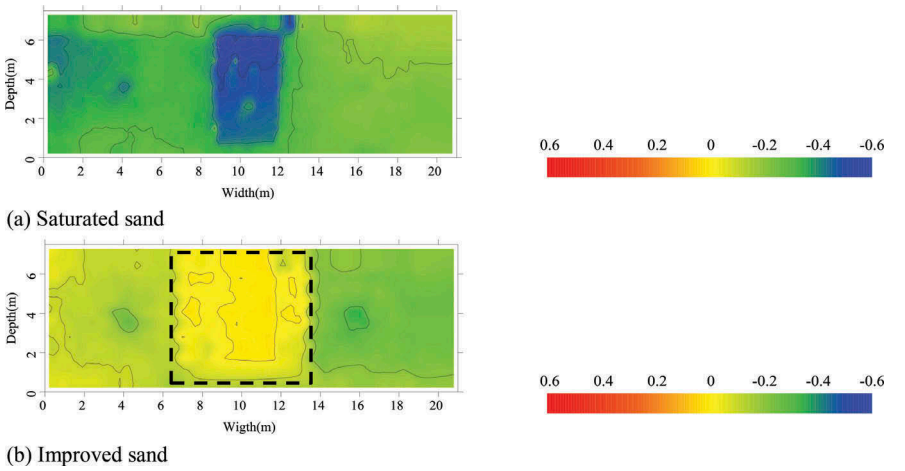

Figure 9. Surface displacement before and after shakings

3.2.5 *Response of structure*

Recorded accelerations of the structure (A-s) and A-2, directly under the structure, are shown in Figure 10 (a) and (b). Acceleration of the structure was the almost same as that of A-2 in the saturated sand but not in the improved sand.

The relationships between cumulative settlement and structure tilt are shown in Figure 11 (a) and (b). As an explanatory note, subscripts *s* and *f* indicate the relationships between total settlement and structure tilt before and after each shaking event. From the result that the amount of settlement gradually decreased even though magnitude of shaking was getting larger in the saturated sand, it is presumed that the ground under the structure became dense by liquefaction. On the other hand, the settlement in the improved sand was less than 0.05 m and the degree of tilt after third shaking decreased compared with the saturated sand. However, the tilt during shakings in the improved sand was large due to the amplification of acceleration.

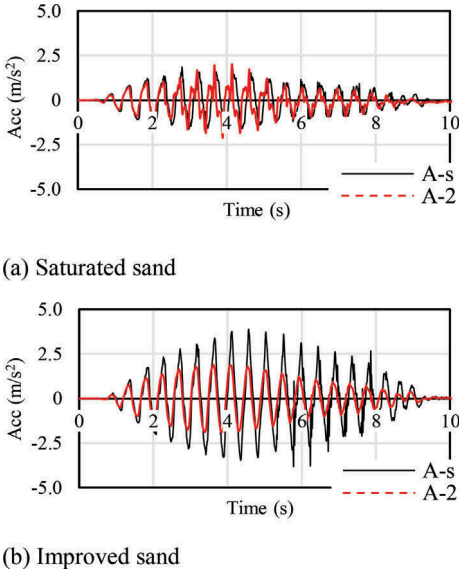

Figure 10. Recorded Acc by A-s and A-2

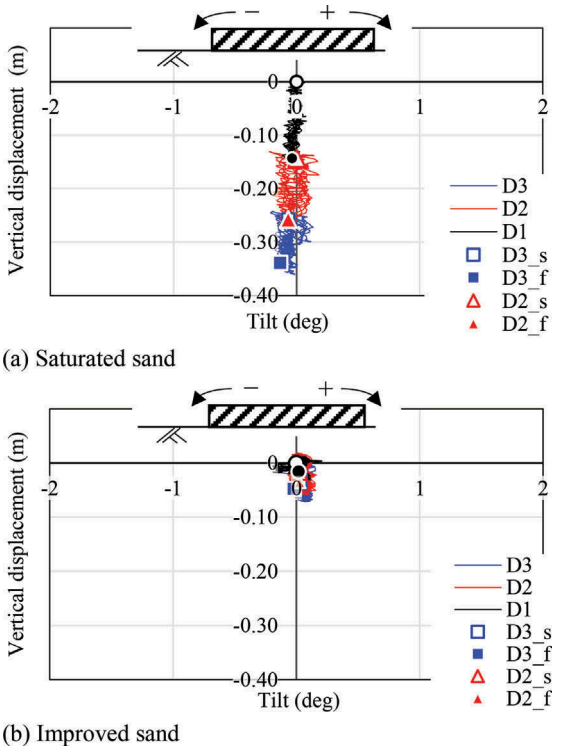

Figure 11. Relatinships between tilt and Vertical displacement

4 CONCLUSIONS

First, in the cyclic triaxial tests, the liquefaction resistance of the improved sand was approximately three times greater than that of the saturated sand. Then, in the centrifuge model tests, while large scale liquefaction occurred in the liquefiable sand during each shaking event, neither decrease in stiffness nor decrease in area of hysteresis due to liquefaction were observed in the improved sand during the second shaking event. In addition, the settlement of improved layer during the shaking evens was small compared with that of the saturated sand.

From these results, the suspension grouting material composed of silica fine particles and fine calcium hydroxide has great potential as a new material for the stabilization of liquefiable sand.

REFERENCES

ChangT. H. & ChangH. W.: Improvement of liquefaction resistance of reclaimed sand in water –an experimental study, J. of Geoengineering, Vol. 2 No. 5, pp. 39-49, 2010.

Dietz, M. & Wood, D. W.: Shaking table evaluation of dynamic soil properties, 4th ICEGE, Paper No. 1196, 2007.

Gallagher, P. M., Pamuk, A. & AbdounT.: Stabilization of liquefiable soils using colloidal silica grout, J. of Materials in Civil Eng., Vol. 19, No. 1, pp. 33-40, 2007.

Moue, T., Uemura, K., Sasaki, T., Nagao, K., Suemasa, N., Itoh, K. & Shimada, S.: A study on strength development of suspended type injection material using microparticles used for liquefaction countermeasure, 8th Int. Conf. GEOMATE, pp. 151-156, 2018.

Okamura, M. & Soga, Y.: Effects of pore fluid compressibility on liquefaction resistance of partially saturated sand, Soils and Foundations, Vol. 46, No. 5, pp. 695-700, 2006.

Yoshimi, Y., Tanaka, K. & Tokimatsu, K.: Liquefaction resistance of a partially saturated sand, Soils and Foundations, Vol. 29, No. 3, pp. 157-162, 1989.